

**Abstract:** A localized spectral analysis of gravity and topography has been applied to the lunar highlands. Assuming that surface and subsurface loads are elastically supported by the lithosphere, the density of the lunar highland crust has been found to vary laterally using Kaguya gravity and LRO topography data. When combined with independent knowledge of crustal density based on compositional data obtained from remote sensing data, the porosity of the upper few kilometers of the crust is estimated to be ~5%. Subsurface loads are found to be small in comparison to surface loads, and the elastic thickness is constrained to be larger than ~5km.

### Why is density important?

#### Geophysical modeling:

- Crustal thickness modeling requires knowledge of the crustal density.
- Lithosphere flexure depends on the density of the crust, load and mantle.

#### Crustal composition:

- Density of crustal materials depends upon composition.

#### Impact crater scaling:

- Impact crater scaling laws depend upon the depth dependence of porosity in the crust.

#### Seismology:

- Seismic wave velocities depend upon density and porosity.

### 1. Lateral variations in crustal density

#### - Constraints from geochemistry and remote sensing

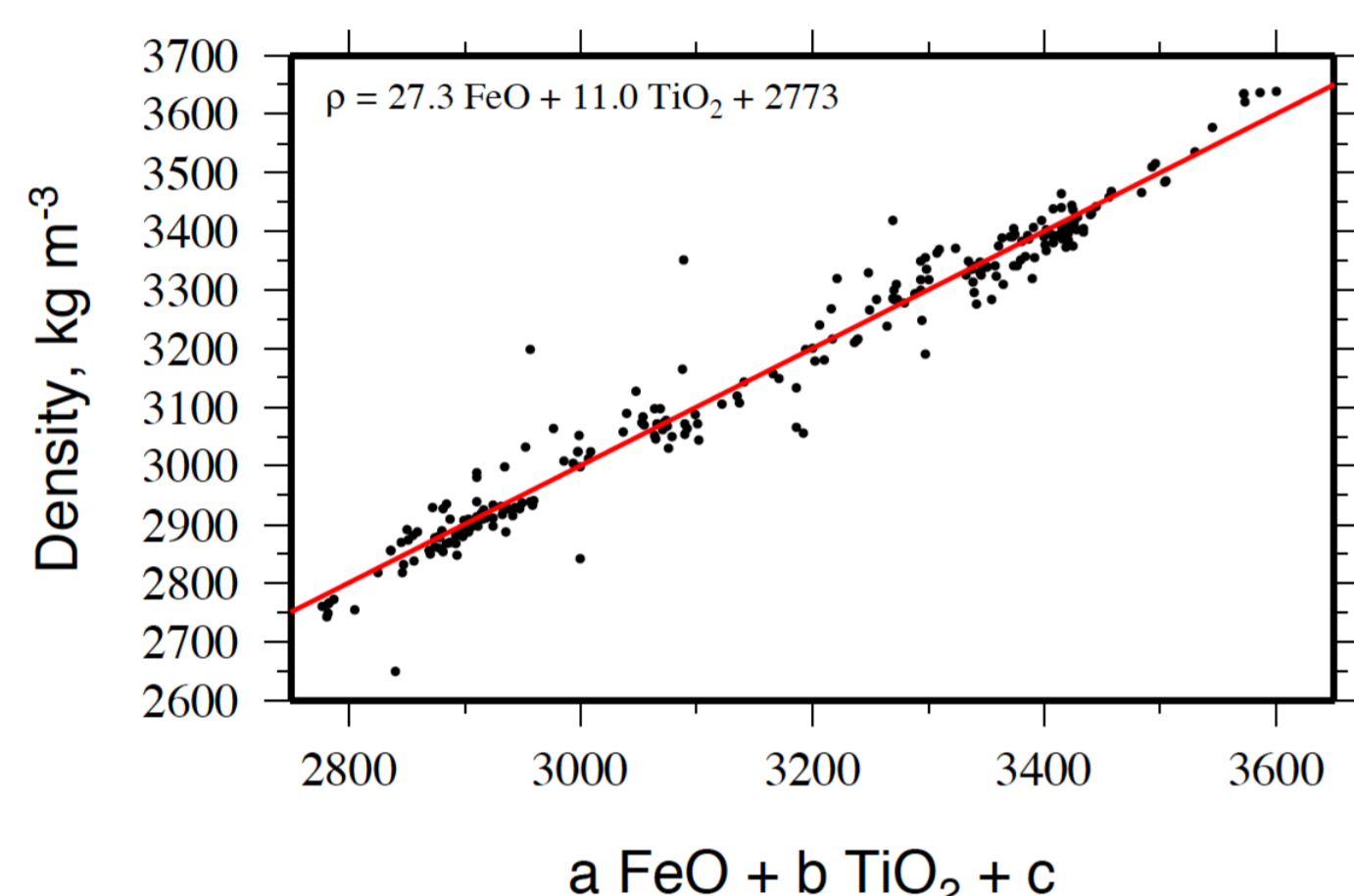


Figure 1: Estimated pore-free densities of lunar samples as a function iron and titanium content.

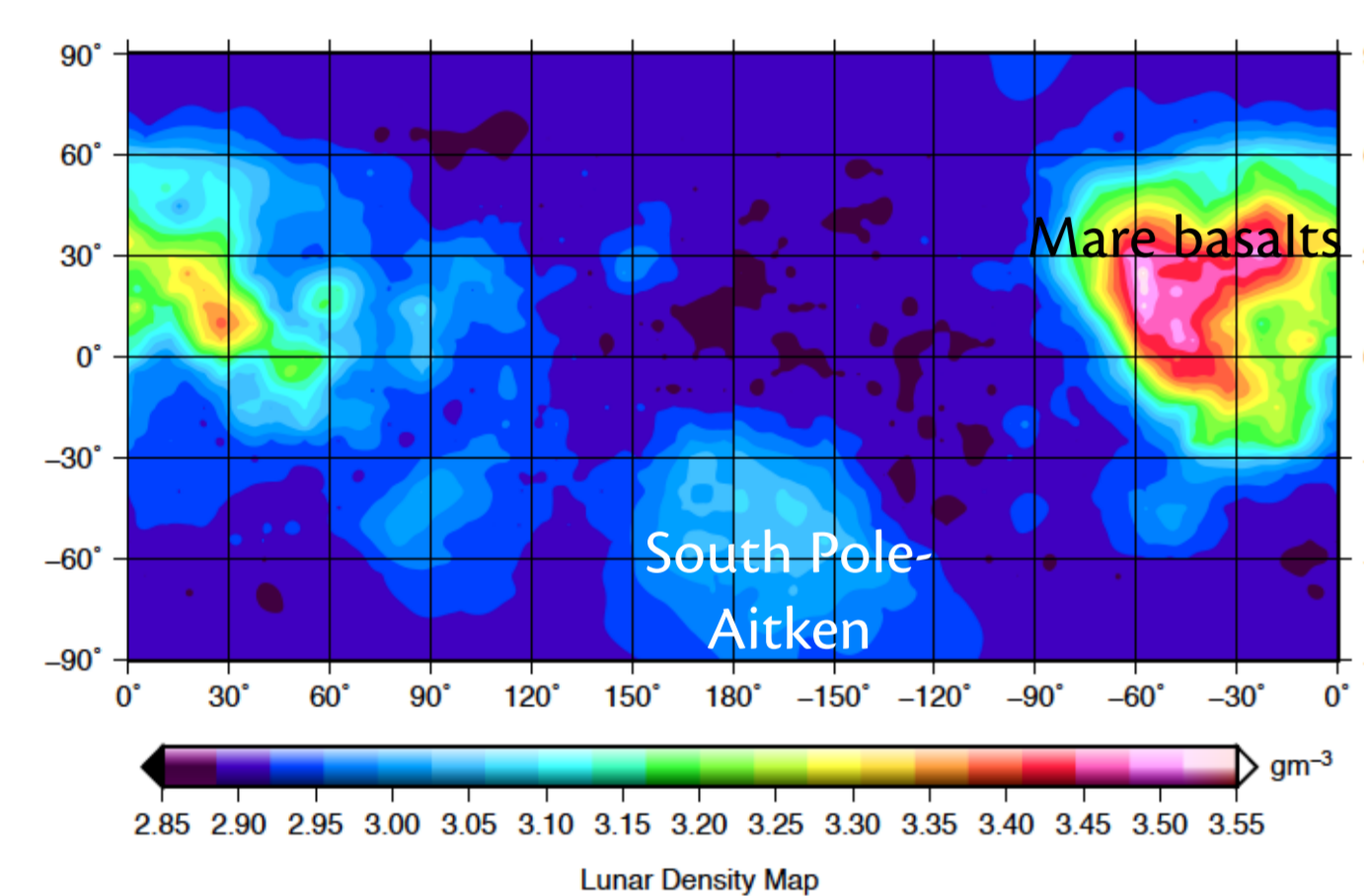


Figure 2: Estimated pore-free density of the lunar surface using Lunar Prospector iron and titanium data.

The Crustal density is predicted to vary by ~300 kg/m<sup>3</sup> in the lunar highlands

### 2. Lateral variations in crustal density

#### - Constraints from gravity and topography

- Gravity and topography are related by the general equation:

$$g_{lm} = Q_{lm} h_{lm}$$

where the linear transfer function  $Q_{lm}$  depends upon a geophysical model of the Moon's interior structure and rheology.

- Calculate the power spectra and cross-power spectrum of gravity and topography, and then calculate the admittance and correlation:

$$\text{Admittance } Z(l) = \frac{S_{hg}(l)}{S_{hh}(l)}$$

$$\text{Correlation } \gamma(l) = \frac{S_{gh}(l)}{\sqrt{S_{hh}(l)S_{gg}(l)}}$$

- The Admittance and correlation can be modeled using a geophysical loading model. For our model described in section 3, these functions depend on crustal density, mantle density, crustal thickness, elastic thickness, and a parameter L that defines the importance of surface and subsurface loading.

$$Z(l), \gamma(l) = f(\rho_c, \rho_m, T_e, T_c, \nu, E, z, L, g, R)$$

# Constraints on the density of the lunar highlands crust from gravity and topography

Qian Huang<sup>1,2</sup>, Mark Wieczorek<sup>1</sup>

<sup>1</sup> Institut de Physique du Globe de Paris, Equipe d'Etudes Spatiales et Planétaire  
4 avenue de Neptune, Saint-Maur 94100 FRANCE (huang@ipgp.fr, wieczor@ipgp.fr)  
<sup>2</sup> Shanghai Astronomical Observatory, Chinese Academy of Science

### 3. Surface and subsurface Load modeling

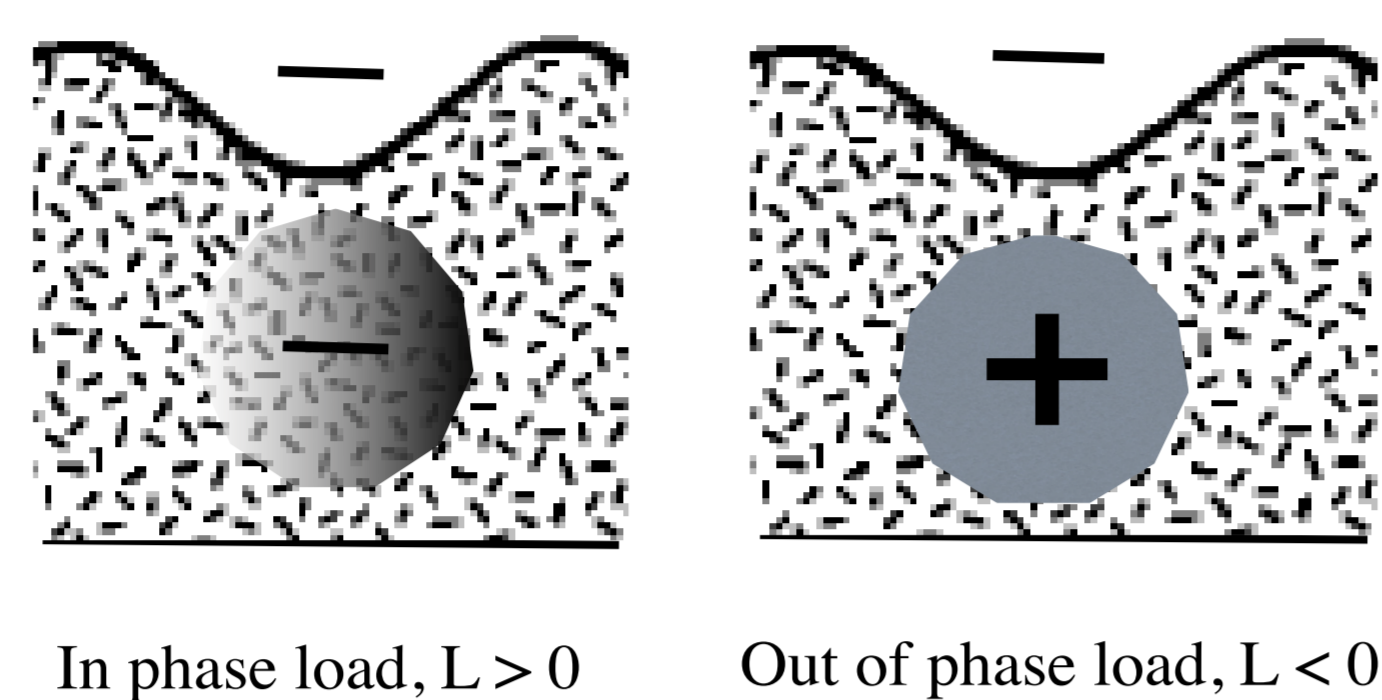


Figure 3. Surface and subsurface loading model.

- In modeling the relation between gravity and topography, we considered the cases where both surface and subsurface loads are emplaced on a thin elastic spherical shell. The loading parameter L is defined as the ratio of the magnitude of material added as a subsurface load, to the combined magnitudes of the surface and subsurface loads. Surface and subsurface loads are assumed to be either in phase (with L being defined as positive) or 180 degrees out of phase (with L being defined as negative). The assumption of surface and subsurface loads being either perfectly correlated or anticorrelated requires correlation function to be either 1 or -1.

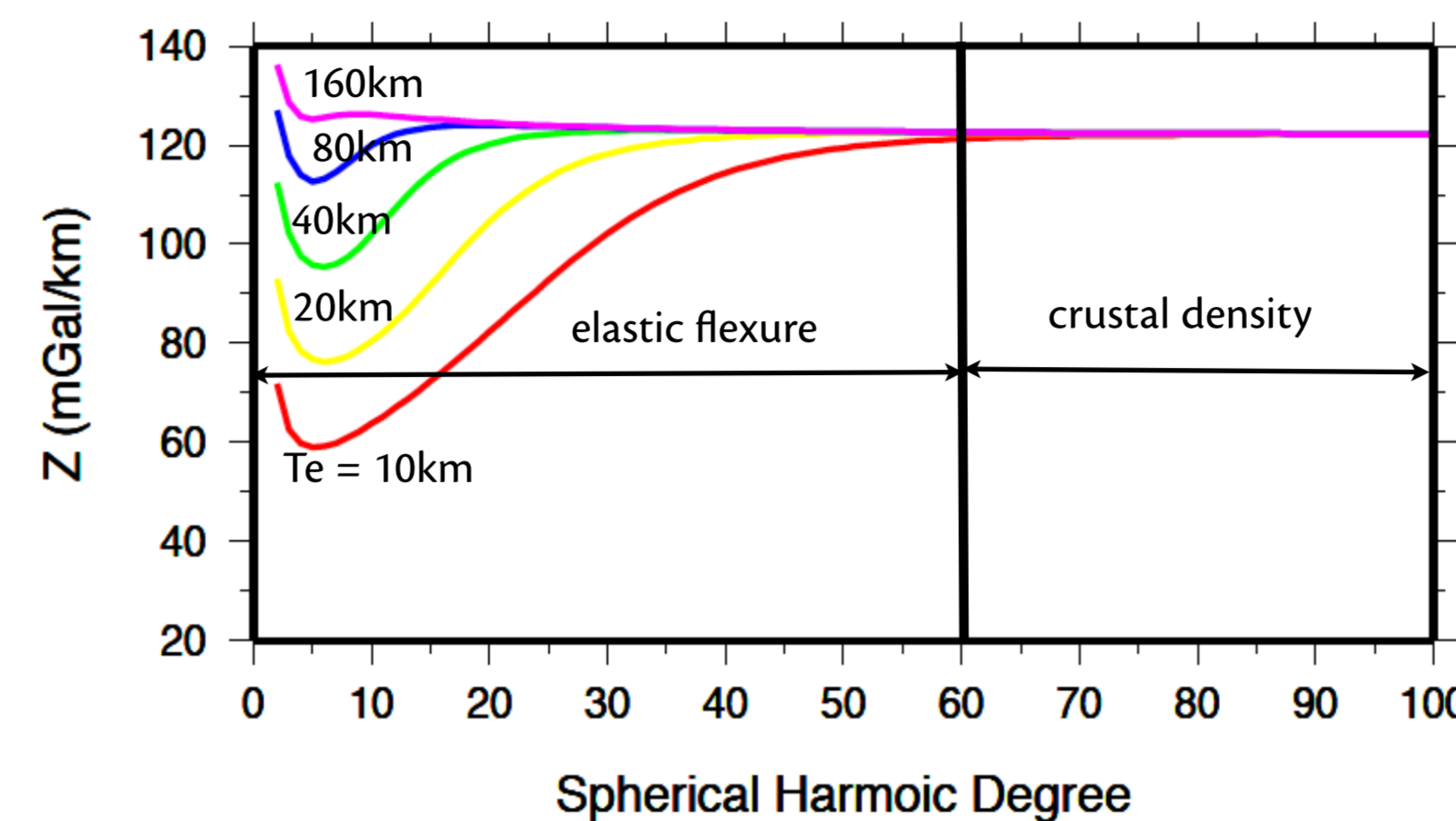
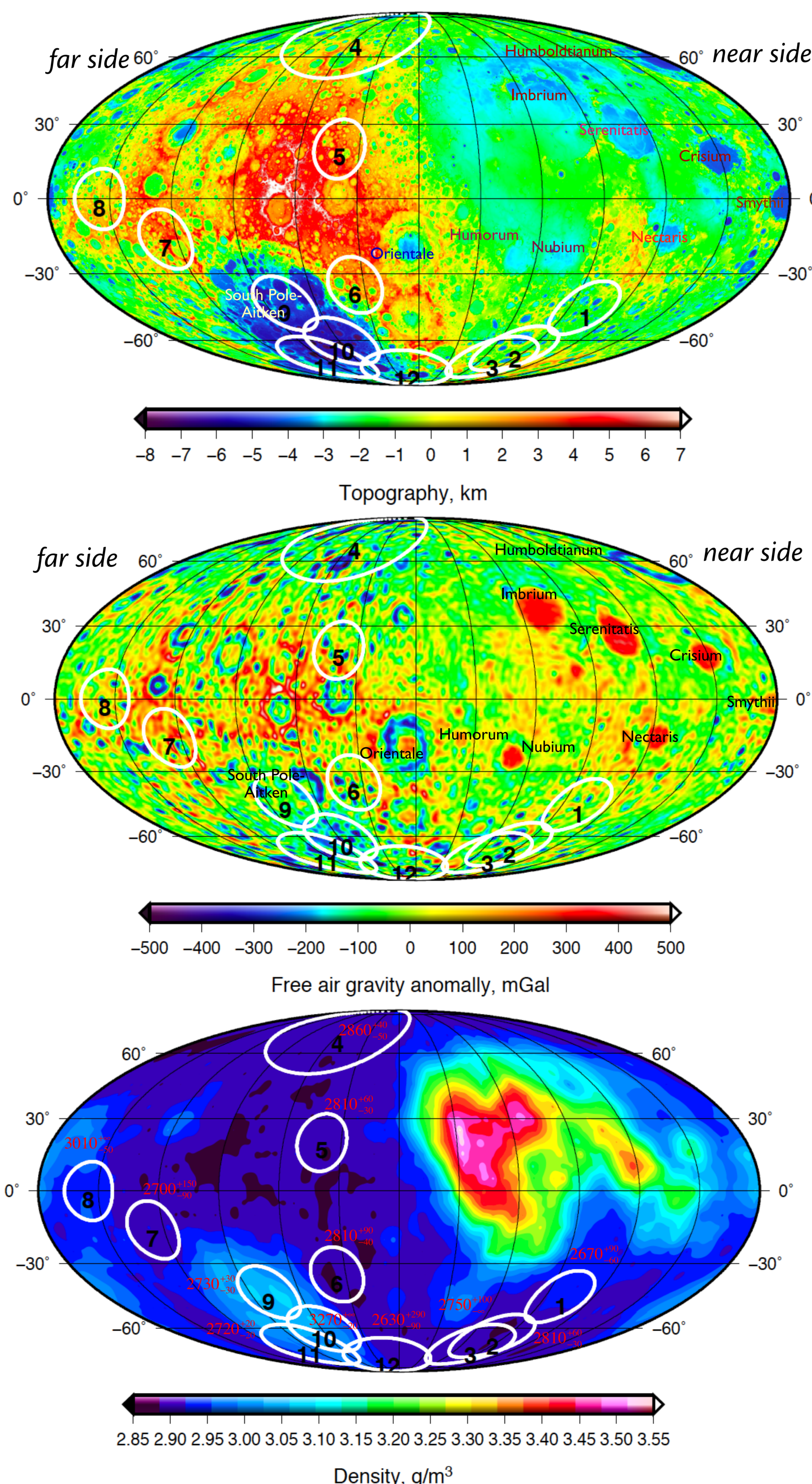


Figure 4. Theoretical admittance spectra for several elastic thicknesses, and for L=0. At high degrees, the admittance approaches a constant value that is proportional to the crustal density.

### 4. Localized spectral analysis on lunar highland regions



#### Modeling Approach:

- 1) Select an homogeneous region of interest.
- 2) Multiply the gravity and topography by a localization window (Wieczorek & Simons (2005, 2007))
- 3) Calculate the localized admittance and correlation.
- 4) Vary  $\rho_c$ ,  $T_e$ ,  $T_c$ ,  $\nu$ , and L to find the best fitting model to the observed admittance and correlation.

### 5. Error estimation

The best fitting model and uncertainties were determined using a multi-step procedure. First, best fitting parameters were determined by minimizing the reduced  $\chi^2$  function:

$$\frac{\chi^2}{\nu}(\rho_c, T_e, L) = \frac{1}{\nu} \sum_{l=l_{min}}^{l_{max}} \left( \frac{Z_l^{obs} - Z_l^{cal}(\rho_c, T_e, L)}{\sigma_l^{obs}} \right)^2$$

where  $\nu$  is the number of degrees of freedom ( $l_{max} - l_{min} - 3$ ). In this step,  $\sigma_l^{obs}$  is a simple estimate of the admittance uncertainty obtained by assuming the localized gravity and topography are linearly related and that the lack of correlation is a result of random noise in the gravity.

In the second step, the uncertainty in the localized admittance was improved upon using a Monte Carlo approach. Given the best fitting model parameters and the published error spectrum of the lunar gravity model, a synthetic gravity field was created that included gravitational noise  $I_{lm}$ ,

$$g_{lm} = Q_{lm}^{bestfit} h_{lm} + I_{lm}^{gravity}$$

The localized admittance was calculated for many random realizations of the noise and compared with the noise free value. The expected uncertainty in the admittance was then estimated as a function of degree using:

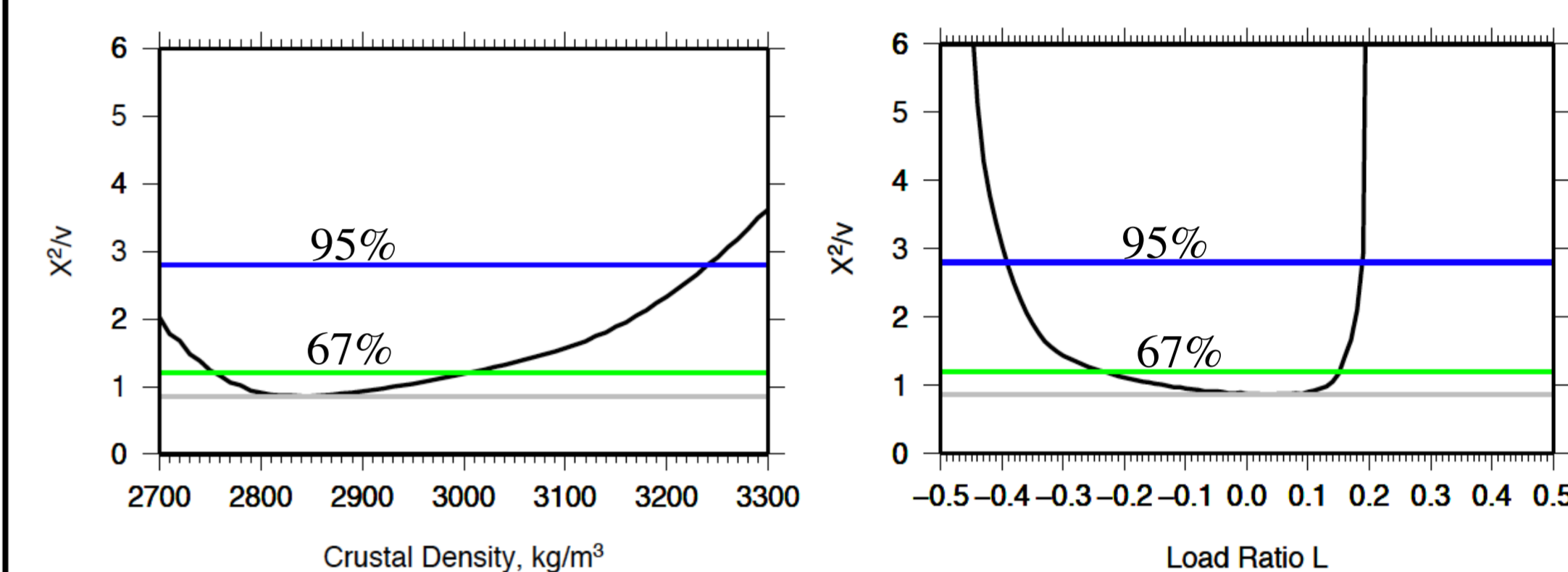
$$\bar{\sigma}_{mc}(l) = \sqrt{\frac{\sum_{i=1}^N (Z_l^{bestfit} - Z_l^{mc})^2}{N}}$$

Next, using the above calculated local admittances that include random noise, the expected probability distribution of the reduced  $\chi^2$  function was calculated,  $P(\chi^2 / \nu < X)$  where

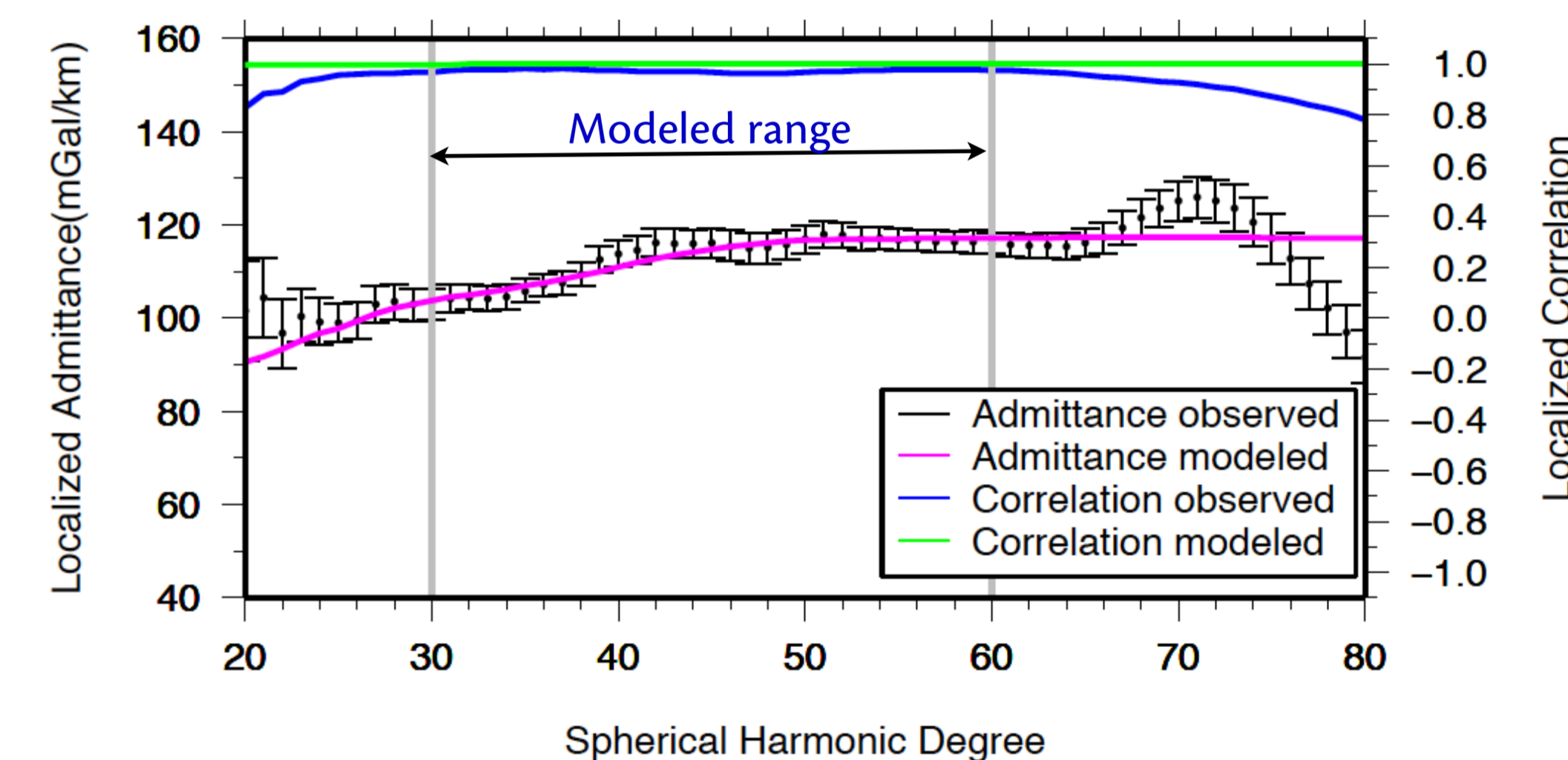
$$\frac{\chi^2}{\nu} = \frac{1}{\nu} \sum_{l=l_{min}}^{l_{max}} \left( \frac{Z_l^{bestfit} - Z_l^{mc}}{\bar{\sigma}_{mc}(l)} \right)^2$$

Finally, the reduced  $\chi^2$  function was recalculated using the improved uncertainties of the admittance and for all values of the model parameters. The allowable range of model parameters were determined using the 67% and 95% confidence intervals.

### 6. Example (210E, 70N)



Minimum misfit as a function of density (left) and load ratio (right), obtained by varying all other model parameters.



Example localized admittance and correlation spectra: the admittance is modeled only where the correlation is approximately unity (as required by our loading model).

### 7. Results

| Region | $\rho_{LP}$ , kg/m <sup>3</sup>    | Model (L=0)                        |                                     | $T_e$ , km                              | Porosity, %                      |                         |
|--------|------------------------------------|------------------------------------|-------------------------------------|---|----------------------------------|-------------------------|
|        |                                    | $\rho_c$                           | L                                   |   |                                  |                         |
| 1      | 2922 <sup>+20</sup> <sub>-30</sub> | 2670 <sup>+20</sup> <sub>-30</sub> | 2640 <sup>+200</sup> <sub>-11</sub> | 0.06 <sup>+0.16</sup> <sub>-0.11</sub>  | 20 <sup>+11</sup> <sub>-11</sub> | 8.62% (5.54 - 10.68%)   |
| 2      | 2894 <sup>+20</sup> <sub>-30</sub> | 2810 <sup>+20</sup> <sub>-30</sub> | 2780 <sup>---</sup>                 | -0.16 <sup>+0.24</sup> <sub>-0.13</sub> | 13 <sup>---</sup>                | 2.90% (0 - 3.94%)       |
| 3      | 2896 <sup>+20</sup> <sub>-30</sub> | 2750 <sup>+20</sup> <sub>-30</sub> | 2810 <sup>---</sup>                 | 0.12 <sup>+0.08</sup> <sub>-0.17</sub>  | 13 <sup>---</sup>                | 5.04% (-1.59%)          |
| 4      | 2899 <sup>+20</sup> <sub>-30</sub> | 2860 <sup>+20</sup> <sub>-30</sub> | 2840 <sup>+20</sup> <sub>-30</sub>  | 0.04 <sup>+0.10</sup> <sub>-0.06</sub>  | 11 <sup>---</sup>                | 2.04% (0 - 5.14%)       |
| 5      | 2896 <sup>+20</sup> <sub>-30</sub> | 2810 <sup>+20</sup> <sub>-30</sub> | 2720 <sup>+20</sup> <sub>-180</sub> | 0.16 <sup>+0.24</sup> <sub>-0.19</sub>  | 30 <sup>---</sup> <sub>-16</sub> | 6.08% (0 - 12.69%)      |
| 6      | 2911 <sup>+20</sup> <sub>-30</sub> | 2810 <sup>+20</sup> <sub>-30</sub> | 2710 <sup>+20</sup> <sub>-180</sub> | 0.15 <sup>+0.06</sup> <sub>-0.04</sub>  | 30 <sup>---</sup> <sub>-17</sub> | 6.90% (0 - 12.74%)      |
| 7      | 2907 <sup>+20</sup> <sub>-30</sub> | 2700 <sup>+20</sup> <sub>-30</sub> | 2660 <sup>+20</sup> <sub>-110</sub> | 0.13 <sup>+0.05</sup> <sub>-0.20</sub>  | 14 <sup>---</sup> <sub>-6</sub>  | 7.12% (1.96 - 10.22%)   |
| 8      | 2943 <sup>+20</sup> <sub>-30</sub> | 3010 <sup>---</sup>                | 2960 <sup>---</sup>                 | 0.08 <sup>+0.03</sup> <sub>-0.18</sub>  | 21 <sup>---</sup> <sub>-19</sub> | 0%                      |
| 9      | 3041 <sup>+20</sup> <sub>-30</sub> | 2730 <sup>+20</sup> <sub>-30</sub> | 2770 <sup>+20</sup> <sub>-30</sub>  | 0.03 <sup>+0.03</sup> <sub>-0.23</sub>  | 21 <sup>---</sup> <sub>-7</sub>  | 10.23% (9.24% - 11.21%) |
| 10     | 3011 <sup>+20</sup> <sub>-30</sub> | 3270 <sup>---</sup>                | 3300 <sup>---</sup>                 | 0.01 <sup>+0.02</sup> <sub>-0.06</sub>  | 6 <sup>---</sup>                 | 0%                      |
| 11     | 2992 <sup>+20</sup> <sub>-30</sub> | 2720 <sup>+20</sup> <sub>-30</sub> | 2670 <sup>+20</sup> <sub>-30</sub>  | 0.06 <sup>+0.08</sup> <sub>-0.17</sub>  | 15 <sup>---</sup> <sub>-2</sub>  | 9.09% (8.42% - 9.76%)   |
| 12     | 2929 <sup>+20</sup> <sub>-30</sub> | 2630 <sup>+20</sup> <sub>-30</sub> | 2680 <sup>+20</sup> <sub>-30</sub>  | 0.11 <sup>+0.13</sup> <sub>-0.17</sub>  | 13 <sup>---</sup> <sub>-4</sub>  | 10.21% (0.3% - 13.28%)  |

$\rho_{LP}$  is estimated pore-free density from Lunar Prospector data,  $\rho_c$  and L are the crustal density and load ratio from the localized admittance analysis. The crustal density was estimated for two models, one with both surface and subsurface loads, and a second with only surface loads (L=0). Comparing with  $\rho_{LP}$  and  $\rho_c$ , we estimate the porosity of the upper few kilometers of the crust.

### 8. Summary and Future work

Crustal density is found to vary laterally by using gravity and topography data. Using gravity-derived bulk density and geochemical density estimates, the porosity of the upper few kilometers of crust is found to be generally less than 10%. Subsurface loads are small in comparison to surface loads and the elastic thickness is less constrained to be larger than ~5 km. In the future, we will try to create a new crustal thickness map that takes into account lateral variations in crustal density. Higher resolution gravity from GRAIL will determine the crustal density to high precision.

Reference: [1] Prettyman, T., et al. (2006), JGR, 90, E12007;  
[2] Wieczorek, M. (2007), Treatise on Geophysics, 10, 165;  
[3] Wieczorek, M., and F. Simons (2005), Geophys. J. Int., 10, 655;  
[4] Belleguic, V., et al. (2005), JGR, 110, E11005;